Minimal geodesics along volume preserving maps, through semi-discrete optimal transport

Quentin Mérigot, Jean-Marie Mirebeau

Minimal geodesics along volume preserving maps, through semi-discrete optimal transport

Quentin Mérigot*† Jean-Marie Mirebeau*‡

May 15, 2015

Abstract

We introduce a numerical method for extracting minimal geodesics along the group of volume preserving maps, equipped with the L^2 metric, which as observed by Arnold [Arn66] solve Euler's equations of inviscid incompressible fluids. The method relies on the generalized polar decomposition of Brenier [Bre91], numerically implemented through semi-discrete optimal transport. It is robust enough to extract non-classical, multi-valued solutions of Euler's equations, for which the flow dimension is higher than the domain dimension, a striking and unavoidable consequence of this model [Shn94]. Our convergence results encompass this generalized model, and our numerical experiments illustrate it for the first time in two space dimensions.

1 Introduction

The motion of an inviscid incompressible fluid, moving in a compact domain $X \subseteq \mathbb{R}^d$, is described by Euler's [Eul65] equations

$$\partial_t v + (v \cdot \nabla) v = -\nabla p \qquad\qquad \operatorname{div} v = 0, \tag{1}$$

coupled with the impervious boundary condition $v \cdot n = 0$ on $\partial\Omega$. Here v denotes the fluid velocity, and p the pressure acts as a Lagrange multiplier for the incompressibility constraint. In Lagrangian coordinates, Euler equations (1) yield the geodesic equations along the group SDiff volume preserving diffeomorphisms of X, equipped with the L^2 metric [Arn66]. Consider an inviscid incompressible fluid flowing during the time interval $[0,1]$, and a map $s^* : X \to X$ giving the final position $s^*(x)$ of each fluid particle initially at position $x \in X$. In this paper, we discretize and numerically investigate a natural approach to reconstruct the intermediate fluid states: look for a minimizing geodesic joining the initial configuration $s_* = \mathrm{Id}$ to the final one s^*

$$\text{minimize} \int_0^1 \|\dot{s}(t)\|^2 dt, \qquad \text{subject to } s(0) = s_*,\ s(1) = s^*, \text{ and } \forall t \in [0,1],\ s(t) \in \mathbb{S}. \tag{2}$$

We denoted by $\mathbb{S} \subseteq L^2(X, \mathbb{R}^d)$ the space of maps preserving the Lebesgue measure on X, which in dimension $d \geq 2$ is the closure of SDiff. Despite this first relaxation, note that the optimized functional in (2) does not penalize the spatial derivatives of s, whereas the constraint involves

*CNRS, Université Paris-Dauphine, UMR 7534, CEREMADE, Paris, France.

†ANR grant TOMMI, ANR-11-BS01-014-01

‡ANR grant NS-LBR, ANR-13-JS01-0003-01

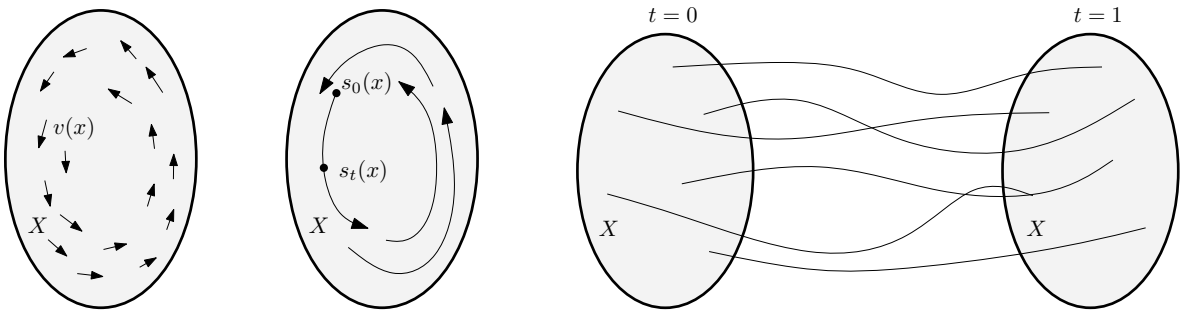

Figure 1: The motion of inviscid incompressible fluids admits three formulations, either (I) Eulerian based on the local speed $v : [0,1] \times X \to \mathbb{R}^d$, (II) Lagrangian based on diffeomorphisms $s(t,\cdot)$ which integrate the speed: $\partial_t s(t,x) = v(t, s(t,x))$, or (III) relaxed as a superposition of individual particles paths $\omega \in \Omega$, weighted by a measure μ.

the jacobian of s. The study of (2) thus requires non-standard variational techniques, reviewed in [FD12].

In dimension $d \geq 3$, the optimization problem (2) needs not have a minimizer in $s \in H^1([0,T], \mathbb{S})$ [Shn94], and minimizing sequences $(s_n)_{n\in\mathbb{N}}$ may instead display oscillations reminiscent of an homogeneization phenomenon. A second relaxation is required, based on generalized flows [Bre89] which allow particles to split and their paths to cross. This surprising behavior is an unavoidable counterpart of the lack of viscosity in Euler's equations, which amounts to an infinite Reynolds number. Generalized flows are also relevant in dimension $d \in \{1,2\}$ if the underlying physical model actually involves a three dimensional domain $X \times [0,\varepsilon]^{3-d}$ in which one neglects the fluid acceleration in the extra dimensions [Bre08]. Consider the space of continuous paths (of fluid particles)

$$\Omega := C^0([0,1], X).$$

Let $e_t(\omega) := \omega(t)$ be the evaluation map at time $t \in [0,1]$, so that $(e_0, e_1)(\omega) = (\omega(0), \omega(1))$. Let also Leb denote the Lebesgue measure restricted to the domain X, normalized for unit mass, and let $f\#\mu$ denote the push-forward of a measure μ by a measurable map f. The geodesic distance (2) admits a convex relaxation, linearizing both the objective and the constraints, and for which the existence of a minimizer is guaranteed. It is posed on probability measures on Ω, called *generalized flows*

$$d^2(s_*, s^*) := \min_{\mu \in \mathrm{Prob}(\Omega)} \int_\Omega \mathcal{A}(\omega) d\mu(\omega), \qquad \text{subject to } \begin{cases} \mathcal{A}(\omega) := \int_0^1 |\dot\omega(t)|^2 dt \\ (\mathrm{e}_0, \mathrm{e}_1)\#\mu = (s_*, s^*)\#\,\mathrm{Leb}, \\ \forall t \in [0,1],\ \mathrm{e}_t\,\#\mu = \mathrm{Leb}\,. \end{cases} \tag{3}$$

Note that the path action $\mathcal{A} : \Omega \to \mathbb{R}_+ \cup \{+\infty\}$, although unbounded, is lower semi-continuous. The first constraint $(\mathrm{e}_0, \mathrm{e}_1)\#\mu = (s_*, s^*)\#\,\mathrm{Leb}$ expresses that moving fluid particles from $s_*(x)$ to $s^*(x)$ for all $x \in X$, or from the origin $\omega(0)$ to the end $\omega(1)$ of the paths $\omega \in \Omega$ as weighted by μ, yields equivalent transport plans. The second constraint $\mathrm{e}_t\,\#\mu = \mathrm{Leb}$ states that the path positions $\omega(t)$, as weighted by μ, equidistribute on X at each time $t \in [0,1]$, which amounts to incompressibility. A classical flow $s \in H^1([0,1], \mathbb{S})$ can be regarded as a generalized flow, with paths $t \mapsto s(t,x)$, weighted by the Lebesgue measure on $x \in X$. Our discretization truly solves (3), rather than (2), and convergence is established in this relaxed setting.

The incompressibility constraint in (1), (2) and (3), gives rise to a Lagrange multiplier, the pressure, which is the *unique* maximizer to a concave optimization problem dual to (3),

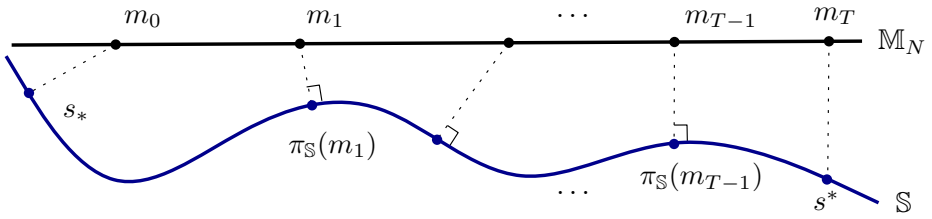

Figure 2: The geodesic distance $d^2(s_*, s^*)$ along the "manifold" $\mathbb{S}$ of volume preserving maps, represented as a blue curve, is estimated (6) as the length of a chain $(m_i)_{i=0}^T$ in the linear subspace $\mathbb{M}_N$, represented as a black line, plus penalizations for the boundary values and the distance from the chain elements to $\mathbb{S}$.

see [Bre93]. The primal (3) may in contrast have several solutions, up to the notable exception [BFS09] of smooth flows in dimension $d = 1$. The pressure is a classical function $p \in L^2_{\text{loc}}(\,]0,T[, \text{BV}(X))$, see [AF07] (which requires the technical assumption that X is a d-dimensional torus). This regularity is sufficient to show that any solution s to (2) (resp. μ-almost any path ω, for any solution μ to (3)) satisfies

$$\partial_{tt} s(t,x) = -\nabla p(t, s(t,x)), \qquad \text{resp.} \quad \ddot{\omega}(t) = -\nabla p(t, \omega(t)). \tag{4}$$

In other words, fluid particles move by inertia, only deflected by the force of pressure. Assume that the pressure hessian is sufficiently small, precisely that

$$\forall t \in [0,1],\ \forall x \in X,\ \nabla^2 p(t,x) \prec \pi^2 \,\mathrm{Id} \tag{5}$$

in the sense of symmetric matrices. Then using the path dynamics equation (4) Brenier [Bre89] showed that the relaxed problem (3) admits a unique minimizer $\mu \in \text{Prob}(\Omega)$, which is *deterministic*: in other words associated to a, possibly non-smooth but otherwise classical, minimizer $s \in H^1([0,T], \mathbb{S})$ of (2). Inequality (5) is sharp, and several families of examples are known for which uniqueness and/or determinism are lost precisely when the threshold (5) is passed. We present §4 the first numerical illustration of this phenomenon.

1.1 Numerical scheme and main results

We introduce a new discretization for the relaxation (3) of the shortest path formulation (2) of Euler equations (1). Our approach is numerically tractable in dimension 2, and is the first to illustrate the transition between classical and generalized solutions occurring at the threshold (5) on the pressure regularity.

For that purpose we need to introduce some notation. Let $\mathbb{M} := L^2(X, \mathbb{R}^d)$, and let $\mathbb{S} \subseteq \mathbb{M}$ be the collection of maps preserving the restriction to X of the Lebesgue measure, denoted by Leb and normalized to have mass 1. For each $N \in \mathbb{N}$ let $\mathcal{P}_N$ be a partition of X into N regions of equal area $1/N$, diameter $\leq C_{\mathcal{P}} N^{-\frac{1}{d}}$, and let $\mathbb{M}_N \subseteq \mathbb{M}$ be the N-dimensional subspace of functions which are piecewise constant on this partition. Given $s_*, s^* \in \mathbb{S}$, discretization parameters $T, N \in \mathbb{N}$, and a penalization factor $\lambda \gg 1$, we solve

$$\mathcal{E}(T,N,\lambda) := \min_{m \in \mathbb{M}_N^{T+1}} T \sum_{0 \leq i < T} \|m_{i+1} - m_i\|^2 + \lambda \bigg(\|m_0 - s_*\|^2 + \|m_T - s^*\|^2 + \sum_{1 \leq i < T} \inf_{s \in \mathbb{S}} \|m_i - s\|^2 \bigg). \tag{6}$$

In all this paper, $\|\cdot\|$ stands for the $L^2(X, \mathbb{R}^n)$ norm, and $|\cdot|$ for the euclidean norm on $\mathbb{R}^n$, for any $n \in \mathbb{N}$. Comparing this with (2), we recognize the standard discretization of the length of the

discrete path $(m_0, \cdots, m_T)$, as well as an implementation by penalization of the boundary value constraints and of the incompressibility constraints. The optimization of (6), seen as a function of $m \in \mathbb{M}_N^{T+1}$, is an $N(T+1)d$-dimensional smooth optimization problem. A quasi-Newton method gave convincing results, see §4, despite the non-convexity of the functional which forbids to guarantee that its global minimum is numerically found.

Before entering the analysis of (6), let us emphasize that the inner-subproblems, the projection of each m_i onto the set $\mathbb{S}$ of measure preserving maps, are numerically tractable thanks to two main ingredients: Brenier's polar factorization [Bre91], and semi-discrete optimal transport. The former states that the distance from any given $m \in \mathbb{M}$ to the set $\mathbb{S}$, is the cost of the transport plan needed to equidistribute on X the image measure of m

$$\inf_{s \in \mathbb{S}} \|m - s\|^2 = W_2^2(m\#\,\mathrm{Leb}, \mathrm{Leb}), \tag{7}$$

where W_2 is the Wasserstein distance for the quadratic transport cost. If $m \in \mathbb{M}_N$, then $m\#\,\mathrm{Leb}$ is the sum of N Dirac measures of mass $1/N$, located at the N values of the piecewise constant map m on the partition $\mathcal{P}_N$. Semi-discrete optimal transport [AHA98, Mer11, Lév14] is a numerical method for computing (7), and more generally the Wasserstein distance between a discrete measure $\eta = \sum_{j=1}^N \eta_j \delta_{x_j}$, and an absolutely continuous measure $\nu = \rho\,\mathrm{Leb}$, with a (typically) piecewise linear density ρ. It is based on Kantorovitch duality

$$W_2^2(\eta, \nu) = \sup_{f \in L^1(\eta)} \int_X f\eta + \int_X g\nu, \qquad \text{where } \forall y \in X,\ g(y) = \inf_{x \in X} |y-x|^2 - f(x), \tag{8}$$

$$= \sup_{f \in \mathbb{R}^N} \sum_{1 \le j \le N} \eta_j f_j + \int_X g\nu, \qquad \text{where } \forall y \in X,\ g(y) = \min_{1 \le j \le N} |y - x_j|^2 - f_j, \tag{9}$$

where (9) is obtained from (8) by setting $f_j = f(x_j)$. Importantly, the conjugate g in (9) is piecewise quadratic on a partition of X, called the Laguerre Diagram of the sites x_j with weights f_j, that is constructible through computational geometry software [cga]. The N-dimensional concave maximization problem (9), which is unconstrained and twice continuously differentiable, is efficiently solved via Newton or quasi-Newton methods. Semi-discrete optimal transport has become a reliable and efficient building block for PDE discretizations [BCMO14].

A second interpretation of the optimization problem (6), closer to (3), involves a generalized flow $\mu \in \mathrm{Prob}(\Omega)$ supported on N trajectories, each piecewise linear with direction changes at times $\{0, 1/T, \cdots, T/T\}$. Let $m = (m_i)_{i=0}^T \in \mathbb{M}_N^{T+1}$, and for each $1 \le j \le N$ let m_i^j be the constant value of m_i on the j-th region of the partition $\mathcal{P}_N$ of X. For each $1 \le j \le N$ let $\omega_j \in \Omega$ be the piecewise linear path with value m_i^j at time i/T, for all $0 \le i \le T$ (see Figure 3). Finally let $\mu \in \mathrm{Prob}(\Omega)$ be the discrete probability measure equidistributed on the set of paths $\{\omega_j;\ 1 \le j \le N\}$. Then (6) rewrites in a form close to (3)

$$\int_\Omega \mathcal{A}(\omega) d\mu(\omega) + \lambda \left(\int_X |m_0(x) - s_*(x)|^2 + |m_T(x) - s^*(x)|^2 dx + \sum_{\substack{1 \le i < T \\ t = i/T}} W_2^2(e_t\#\mu, \mathrm{Leb}) \right). \tag{10}$$

Indeed, the first energy term satisfies

$$\int_\Omega \mathcal{A}(\omega) d\mu(\omega) = \frac{1}{N} \sum_{1 \le j \le N} \int_0^1 |\dot\omega_j(t)|^2 dt = \frac{T}{N} \sum_{\substack{0 \le i < T \\ 1 \le j \le N}} |m_{i+1}^j - m_i^j|^2 = T \sum_{0 \le i < T} \|m_{i+1} - m_i\|^2.$$

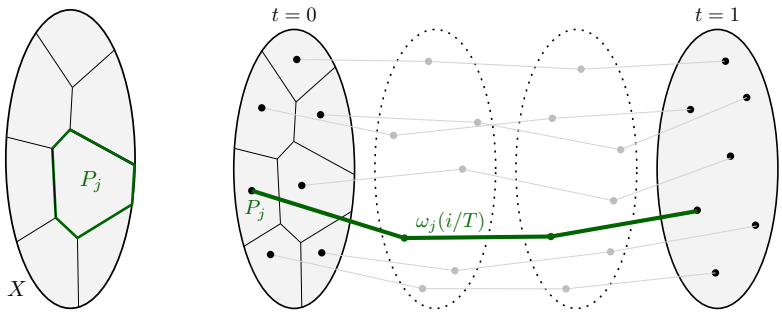

Figure 3: (Left) A partition $\mathcal{P}_N$ cuts the domain X into N region of equal area and roughly isotropic shape. (Right) To a sequence $(m_i)_{i=0}^T \in \mathbb{M}_N^{T+1}$ one can associate N piecewise linear paths $(\omega_j)_{j=1}^N$, by interpolating the map values at the times $\{0, 1/T, \cdots, T/T\}$ for each region of the partition $\mathcal{P}_N$.

The penalized integral term in (10) equals $\|m_0 - s_*\|^2 + \|m_T - s^*\|^2$ from (6). It is the cost of the transport plan on X^2 mapping $(m_0(x), m_T(x))$ to $(s_*(x), s^*(x))$ for all $x \in X$, which sends $(\mathrm{e}_0, \mathrm{e}_1)\#\mu = (m_0, m_T)\#\,\mathrm{Leb}$ onto $(s_*, s^*)\#\,\mathrm{Leb}$, and thus enforces the proximity of these two couplings on X^2 as required in (3). The other penalized terms $W_2^2(\mathrm{e}_t\,\#\mu, \mathrm{Leb})$ account for the incompressibility of μ at time $t = i/T$, $1 \leq i < T$, and by (7) are equal to $\inf_{s\in\mathbb{S}} \|m_i - s\|^2$ from (6).

Summarizing, the geodesic formulation of Euler equations (2) has a rather surprising relaxation (3), looking a-priori unphysical: fluid particles may split and cross. Yet the natural discretizations (6) and (10) of these two formulations are actually *identical*. The classical and generalized interpretations are also at the heart of our main result.

Theorem 1.1. *Let $s_*, s^* \in \mathbb{S}$, let $T, N \in \mathbb{N}$, and $\lambda \geq 0$. The relaxed geodesic distance* (3) *and the discretized minimum* (6) *satisfy*

$$\mathcal{E}(T, N, \lambda) \leq d(s_*, s^*) + \mathcal{O}(T h_N^2 \lambda),$$

- *(Classical estimate) with $h_N = N^{-\frac{1}{d}}$, if the classical geodesic distance* (2) *equals the relaxed distance* (3)*, and admits a minimizer with regularity $s \in L^\infty([0,1], H^1(X))$.*
- *(Relaxed estimate) with $h_N = N^{-\frac{1}{2d}}$ (resp. $N^{-\frac{1}{2}}\sqrt{\ln N}$ if $d = 1$), if the pressure field gradient ∇p is Lipschitz on $[0,1] \times X$, and the boundary data s_*^{-1}, s^* are Lipschitz on X.*

Recall that the classical (2) and relaxed (3) distances are automatically equal in dimension $d \geq 3$, and that the pressure field gradient ∇p is uniquely determined by the boundary values s_*, s^*.

The decay rate $h_N = N^{-\frac{1}{D}}$ in Theorem 1.1 is actually tied to the dimension $D_{\mathrm{quant}}(\mu)$ of the generalized flow $\mu \in \mathrm{Prob}(\Omega)$ minimizing (3), see Definition 3.1. The flow associated to a classical solution has dimension d, since the particle trajectories are determined by their initial position $x \in X \subseteq \mathbb{R}^d$. The trajectories of a generalized flow obey a second order ordinary differential equation (4) and are thus determined by their initial position and velocity $(x, v) \in X \times \mathbb{R}^d \subseteq \mathbb{R}^{2d}$, provided Cauchy-Lipschitz's theorem applies. The generalized flow dimension is thus $2d$ in the worst case, but intermediate dimensions $d < D < 2d$ are also common, see §4.

Theorem 1.1 does not tell how to choose the constraint penalization parameter λ. The next proposition shows that the quantity $\mathcal{E}'(T, N, \lambda) := (1 + 4T/\lambda)\mathcal{E}(T, N, \lambda)$ arises naturally in error

estimates, which suggests to choose $\lambda = h_N^{-1} = N^{\frac{1}{D}}$ so that

$$\mathcal{E}'(T, N, \lambda) = d^2(s_*, s^*) + \mathcal{O}(T/\lambda + T h_N^2 \lambda) = d^2(s_*, s^*) + \mathcal{O}(T N^{-\frac{1}{D}}). \tag{11}$$

Proposition 1.2. *Let $m = (m_i)_{i=0}^T \in \mathbb{M}_N^{T+1}$ be a minimizer of (6).*

- *(Classical construction) Let $(s_i)_{i=0}^T$ be the chain of incompressible maps defined by: $s_0 = s_*$, $s_T = s^*$, and s_i is a projection of m_i onto $\mathbb{S}$ for all $1 \leq i < T$. Then*

$$T \sum_{0 \leq i < T} \|s_{i+1} - s_i\|^2 \leq \mathcal{E}'(T, N, \lambda).$$

- *(Relaxed construction) Let $\mu \in \mathrm{Prob}(\Omega)$ be the generalized flow built from $(m_i)_{i=0}^T$ as in (10). Then*

$$\int_0^1 W_2^2(\mathrm{e}_t \#\mu, \mathrm{Leb})\, dt \leq \frac{1}{4T^2} \mathcal{E}'(T, N, \lambda).$$

  As a result, let $(N_T, \lambda_T)_{T \in \mathbb{N}}$ be such that $\mathcal{E}'(T, N_T, \lambda_T) \to d(s_*, s^*)$ as $T \to \infty$. Then a subsequence of the associated flows $(\mu_T)_{T \in \mathbb{N}}$ weak- converges to a minimizer of (3).*

Outline. Theorem 1.1 is established §2.1 (Classical estimate) and §3 (Relaxed estimate). Proposition 1.2 is proved §2.2. Numerical experiments are presented §4.

Remark 1.3 (Monge-Ampere gravitation)**.** *Some models of reconstruction of the early universe [Bre11] involve actions of a form closely related to our discrete energy functional (6), for the parameter value $\lambda = 2$:*

$$\int_0^1 \left(\frac{1}{2} \|\dot{m}(t)\|^2 + \inf_{s \in \mathbb{S}} \|m(t) - s\|^2 \right) dt.$$

2 Classical analysis

We establish Theorem 1.1 (Classical estimate) in §2.1, and prove Proposition 1.2 in §2.2. The optimization parameters $(T, N, \lambda, s_*, s^*)$ are fixed in this section.

2.1 Upper estimate of the discretized energy

Following the assumption of Theorem 1.1 (Classical estimate), we consider a minimizer of the shortest path problem (2), and assume that it has regularity $s \in L^\infty([0,1], H^1(X))$. Define $s_i := s(i/T)$ for all $0 \leq i \leq T$, and note that $s_0 = s_*$, $s_T = s^*$. Let also $m_i := \mathbb{P}_N(s_i)$, for all $0 \leq i \leq T$, where $\mathbb{P}_N : \mathbb{M} \to \mathbb{M}_N$ denotes the orthogonal projection. We denote by $h_N := N^{-\frac{1}{d}}$ the discretization scale, and recall that each region of the partition $\mathcal{P}_N$ of X has area $1/N$ and diameter $\leq C_{\mathcal{P}} h_N$.

Let s_i^P denote the mean of s_i on the region P of the partition $\mathcal{P}_N$, for all $0 \leq i \leq T$. Then

$$\|s_i - m_i\|^2 = \sum_{P \in \mathcal{P}_N} \int_P |s_i(x) - s_i^P|^2 dx \leq C_{\mathrm{sb}} (C_{\mathcal{P}} h_N)^2 \sum_{P \in \mathcal{P}_N} \int_P |\nabla s_i(x)|^2 dx = C h_N^2 \|\nabla s_i\|^2, \tag{12}$$

where the Sobolev inequality constant C_{sb} only depends on the dimension, and $C := C_{\mathrm{sb}} C_{\mathcal{P}}^2$. Recall that, in all this paper, $\|\cdot\|$ stands for the $L^2(X, \mathbb{R}^n)$ norm, and $|\cdot|$ for the euclidean norm

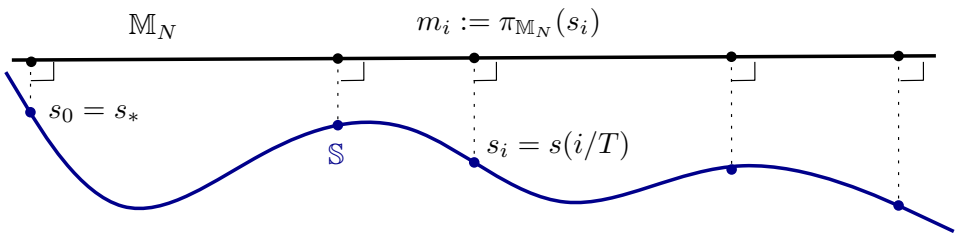

Figure 4: Theorem 1.1 (classical estimate) is based projecting the measure preserving maps $(s_i)_{i=0}^T \in \mathbb{S}^{T+1}$ onto the finite dimensional space $\mathbb{M}_N$, a procedure symmetric the projection of $(m_i)_{i=1}^{T-1} \in \mathbb{M}_N^{T-1}$ onto $\mathbb{S}$ involved in the discrete energy optimization (6), see Figure 2.

on $\mathbb{R}^n$, for any integer $n \geq 1$. The map $\mathbb{P}_N$ is 1-Lipschitz, as the orthogonal projection onto the convex set $\mathbb{M}_N$. Hence for any $0 \leq i < T$

$$\|m_i - m_{i+1}\|^2 \leq \|s_i - s_{i+1}\|^2 \leq \frac{1}{T} \int_{\frac{i}{T}}^{\frac{i+1}{T}} \|\dot{s}(t)\|^2 dt. \tag{13}$$

Summing (12) and (13) over $0 \leq i \leq T$ we obtain

$$\begin{aligned}
\mathcal{E}(T, N, \lambda) &\leq T \sum_{0 \leq i < T} \|m_{i+1} - m_i\|^2 + \lambda \sum_{0 \leq i \leq T} \|m_i - s_i\|^2 \\
&\leq \sum_{0 \leq i < T} \int_{\frac{i}{T}}^{\frac{i+1}{T}} \|\dot{s}(t)\|^2 dt + \lambda \sum_{0 \leq i \leq T} C h_N^2 \|\nabla s_i\|^2 \\
&\leq d^2(s_*, s^*) + C' T h_N^2 \lambda,
\end{aligned}$$

where $C' = C\|s\|_{L^\infty([0,1], H^1(X))}$, which concludes the proof.

2.2 Length of a chain of incompressible maps

Proposition 1.2 (Classical construction) immediately follows from Lemma 2.1 below, which is general and could be used to approximate geodesics on any manifold $\mathbb{S}$ embedded in a Hilbert space $\mathbb{M}$, internally approximated by subspaces $\mathbb{M}_N$. It relies on a the following identity, valid for any elements a, b of a Hilbert space, and any $\varepsilon > 0$:

$$(1 + \varepsilon)^{-1} \|a + b\|^2 \leq \|a\|^2 + \varepsilon^{-1} \|b\|^2. \tag{14}$$

Indeed subtracting the LHS to the RHS of (14) we obtain $(1 + \varepsilon)^{-1} \|\varepsilon^{\frac{1}{2}} a - \varepsilon^{-\frac{1}{2}} b\|^2 \geq 0$.

Lemma 2.1. *For any $T \in \mathbb{N}^*$, any penalization $\lambda > 0$, and any $(m, s) \in (\mathbb{M} \times \mathbb{S})^{T+1}$ one has*

$$T \sum_{0 \leq i < T} \|s_{i+1} - s_i\|^2 \leq (1 + 4T/\lambda) \left[T \sum_{0 \leq i < T} \|m_{i+1} - m_i\|^2 + \lambda \sum_{0 \leq i \leq T} \|m_i - s_i\|^2 \right]. \tag{15}$$

Proof. Let $0 \leq i < T$. Choosing $a := s_{i+1} - s_i$, and $b := m_{i+1} - m_i - a$, we obtain

$$\begin{aligned}
(1 + \varepsilon)^{-1} \|m_{i+1} - m_i\|^2 &\leq \|s_{i+1} - s_i\|^2 + \varepsilon^{-1} \|(s_i - m_i) - (s_{i+1} - m_{i+1})\|^2 \\
&\leq \|s_{i+1} - s_i\|^2 + 2\varepsilon^{-1} (\|s_i - m_i\|^2 + \|s_{i+1} - m_{i+1}\|^2).
\end{aligned}$$

Summing over $0 \le i < T$ yields

$$(1+\varepsilon)^{-1} \sum_{0\le i<T} \|m_{i+1}-m_i\|^2 \le \sum_{0\le i<T} \|s_{i+1}-s_i\|^2 + 2\varepsilon^{-1} \sum_{0\le i\le T} \alpha_i \|s_i - m_i\|^2,$$

with $\alpha_0 = \alpha_T = 1$, $\alpha_i = 2$ otherwise. Choosing $\varepsilon = 4T/\lambda$ concludes the proof. □

The second point of Proposition 1.2 is based on (14) as well. Indeed, let $(m_i)_{i=0}^T$ be minimizers of (6), let $0 \le i < T$, and let $t = (i+\alpha)/T$ with $0 \le \alpha \le 1$. Then for any $\varepsilon > 0$

$$W_2^2(\mathrm{e}_t \#\mu, \mathrm{Leb}) = \inf_{s\in\mathbb{S}} \|(1-\alpha)m_i + \alpha m_{i+1} - s\|^2 \le (1+\varepsilon)\left(\|\alpha(m_{i+1}-m_i)\|^2 + \varepsilon^{-1} \inf_{s\in\mathbb{S}} \|m_i - s\|^2 \right)$$

Integrating over $t \in [0,1]$, using that either $\alpha \le 1/2$ or $1-\alpha \le 1/2$, and choosing $\varepsilon = 4T/\lambda$, we obtain as announced

$$\int_0^1 W_2^2(\mathrm{e}_t \#\mu, \mathrm{Leb}) dt \le \frac{1+\varepsilon}{T} \sum_{0\le i<T} \left(\frac{1}{4}\|m_{i+1}-m_i\|^2 + \varepsilon^{-1} \inf_{s\in\mathbb{S}} \|m_i - s\|^2 \right) = \frac{1}{4T^2}\mathcal{E}'(T,N,\lambda).$$

Finally, the convergence claim for the minimizing chain $(\mu_T)_{T\in\mathbb{N}}$ results from classical arguments. (i) The weak-* lower semi-continuity of the energy $\mu \mapsto \int_\Omega \mathcal{A}(\omega) d\mu(\omega)$ on $\mathrm{Prob}(\Omega)$, which follows from the lower semi-continuity of the action $\mathcal{A} : \Omega \to \mathbb{R}_+ \cup \{\infty\}$. (ii) The weak-* sequential compactness of $\{\mu \in \mathrm{Prob}(\Omega);\ \int_\Omega \mathcal{A}(\omega) d\mu(\omega) \le K\}$ for any constant K, see [Bre93]. (iii) The weak-* continuity of $\mu \mapsto W_2^2((\mathrm{e}_0,\mathrm{e}_1)\#\mu, (s_*,s^*)\#\,\mathrm{Leb})$, a quantity bounded for μ_T by $\|m_0 - s_*\|^2 + \|m_T - s^*\|^2 \le \mathcal{E}(T,N_T,\lambda_T)/\lambda_T \to 0$ as $T \to \infty$. (iv) The weak-* lower semi-continuity of $\mu \mapsto \int_0^1 W_2^2(\mathrm{e}_t\#\mu, \mathrm{Leb})\, dt$, which follows from Fatou's lemma and the continuity of $\mu \mapsto W_2^2(\mathrm{e}_t\#\mu, \mathrm{Leb})$ for any $t \in [0,1]$.

3 Relaxed analysis

We prove Theorem 1.1 (Relaxed estimate), using a quantization of the generalized flow minimizing the relaxed geodesic distance (3). This quantization is a counterpart of the partition $\mathcal{P}_N$ of the domain (X, Leb) used for the classical estimate §2.1, which amounts to quantize the initial positions of the fluid particles. Let δ_x denote the Dirac probability measure concentrated at a point x.

Definition 3.1. *Let $\mathbb{H}$ be a metric space, let μ be a probability measure on $\mathbb{H}$, and let $\Gamma \subseteq \mathbb{H}$. For all $N \ge 1$ denote, with W_2 the Wasserstein distance for the quadratic transportation cost*

$$h_N(\mu) := \inf_{\omega\in\mathbb{H}^N} W_2\Big(\mu,\ \frac{1}{N}\sum_{1\le i\le N} \delta_{\omega_i}\Big), \quad r_N(\Gamma) := \inf_{\omega\in\mathbb{H}^N} \min\Big\{ r \ge 0;\ \Gamma \subseteq \bigcup_{1\le i\le N} \overline{B}(\omega_i, r)\Big\}.$$

The quantization dimension of μ, and the box dimension of Γ, are defined by

$$D_{\mathrm{quant}}(\mu) := \limsup_{N\to\infty} \frac{\ln N}{-\ln h_N(\mu)}, \qquad D_{\mathrm{box}}(\Gamma) := \limsup_{N\to\infty} \frac{\ln N}{-\ln r_N(\Gamma)}.$$

The decay rate of h_N is directly involved in the announced result Theorem 1.1. We estimate it using an elementary result of quantization theory, and refer to [GG92] for more details on this rich subject. Note that the (upper) box dimension D_{box} is a variant of the Haussdorff dimension, in which the set of interest if covered by balls of *equal* radius. Box and Haussdorff

dimension coincide for compact manifolds, but differ in general. For instance, all countable sets have Haussdorff dimension zero, whereas one can check that

$$D_{\mathrm{box}}\Big(([0,1]\cap\mathbb{Q})^d\Big)=d, \qquad\qquad D_{\mathrm{box}}\left(\left\{\frac{1}{n};\, n\in\mathbb{N}^*\right\}\right)=\frac{1}{2}.$$

Proposition 3.2. *Let $\mathbb{H}$ be a metric space, and let $\mu\in\mathrm{Prob}(\mathbb{H})$ be supported on a set Γ. Then $D_{\mathrm{quant}}(\mu)\leq\max\{2,D_{\mathrm{box}}(\Gamma)\}$. More precisely for any $D>0$, one has as $N\to\infty$*

$$r_N(\Gamma)=\mathcal{O}(N^{-\frac{1}{D}}) \quad\Rightarrow\quad h_N(\mu)=\mathcal{O}\begin{cases}N^{-\frac{1}{D}} & \text{if } D>2,\\ N^{-\frac{1}{2}}\sqrt{\ln N} & \text{if } D=2,\\ N^{-\frac{1}{2}} & \text{if } D<2.\end{cases} \tag{16}$$

Proof. Let $N\in\mathbb{N}$ be fixed. For each $1\leq i\leq N$ let $M_i\subseteq\mathbb{H}$ be a set of i points such that $\Gamma\subseteq\cup_{\omega\in M_i}\overline{B}(\omega,2r_i)$, with $r_i:=r_i(\Gamma)$. We construct a sequence of points $\omega_i\in\mathbb{H}$, and an increasing sequence of measures ρ_i supported on Γ and of mass i/N, inductively starting with $i=N$ and finishing with $i=1$. Initialization: $\rho_N:=\mu$.

Induction: for each $1\leq i\leq N$, we construct ω_i and ρ_{i-1} in terms of ρ_i. Let indeed $\omega_i\in M_i$ be such that $B_i:=\overline{B}(\omega_i,2r_i)$ satisfies $\rho_i(B_i)\geq 1/N$. Such a point exists since $|\rho_i|=i/N$, $\#(M_i)=i$, and $\mathrm{supp}(\rho_i)\subseteq\Gamma$. Then let $\rho_{i-1}:=\rho_i-\frac{1}{N\rho_i(B_i)}\rho_i$, so that $\rho_i-\rho_{i-1}$ is a non-negative measure of mass $\frac{1}{N}$ supported on $\overline{B}_i$. One has

$$h_N(\mu)^2\leq W_2^2\left(\mu,\frac{1}{N}\sum_{1\leq i\leq N}\delta_{\omega_i}\right)\leq\sum_{1\leq i\leq N}W_2^2\left(\rho_i-\rho_{i-1},\frac{1}{N}\delta_{\omega_i}\right)\leq\frac{1}{N}\sum_{1\leq i\leq N}(2r_i)^2.$$

The comparison (16) of the decay rates of $h_N(\mu)$ and $r_N(\Gamma)$ immediately follows. Finally the comparison of the dimensions follows from (16). □

We now specialize the choice of μ, Γ and $\mathbb{H}$. Let $\mu\in\mathrm{Prob}(\Omega)$ be a generalized flow minimizing the relaxed geodesic distance (3). This measure is concentrated on the set Γ of paths obeying Newton's second law of motion

$$\Gamma:=\{\omega\in C^2([0,1],X);\,\forall t\in[0,1],\ \ddot{\omega}(t)=-\nabla p(t,\omega(t))\},$$

where the pressure gradient $\nabla p:[0,1]\times X\to\mathbb{R}^d$ is assumed, following the assumptions of Theorem 1.1, to have Lipschitz regularity. We regard Γ as embedded in the Hilbert space $\mathbb{H}:=H^1([0,1],\mathbb{R}^d)$, which plays a natural role in the problem of interest (3) and is equipped with the norm

$$\|\omega\|_{\mathbb{H}}^2:=\left|\int_0^1\omega\right|^2+\int_0^1|\dot{\omega}|^2.$$

Note that $\mathbb{H}$ continuously embeds in $C^0(\Omega,\mathbb{R}^d)$, hence the evaluation maps $\mathrm{e}_t:\mathbb{H}\to\mathbb{R}^d$ are continuous with a common Lipschitz constant denoted C_{e}.

Lemma 3.3. *The set Γ is compact. Furthermore the map $\Gamma\to X\times\mathbb{R}^d:\omega\mapsto(\omega(0),\dot{\omega}(0))$ is bijective and bi-Lipschitz onto its image.*

Proof. The result follows from Cauchy-Lipschitz's theorem for ordinary differential equations, and the compactness of X. □

The image of the generalized flow μ by the map of Lemma 3.3, namely initial position and speed, is often called a minimal measure [BFS09]. Since there is no ambiguity, we denote $h_N := h_N(\mu)$. The constants c, C, C' appearing in the estimates below only depend on the dimension d.

Corollary 3.4. *One has $h_N = \mathcal{O}(N^{-\frac{1}{2d}})$ (resp. $\mathcal{O}(N^{-\frac{1}{2}}\sqrt{\ln N})$ if $d = 1$.)*

Proof. By Lemma 3.3, the set Γ is in bi-Lipschitz bijection with a compact set $K \subseteq \mathbb{R}^{2d}$. Hence $r_N(\Gamma) \leq C r_N(K) \leq C' N^{-\frac{1}{2d}}$, and the upper estimate follows from (16). □

The quantization scale h_N is also bounded below, and is minimal for classical solutions.

Lemma 3.5. *There exists $c > 0$ such that $h_N \geq cN^{-\frac{1}{d}}$ for all $N > 0$. If the generalized flow μ in fact represents a classical solution s to Euler's equations, and $\nabla \dot{s}$ is bounded on $[0,1] \times X$, then this lower estimate is sharp: $h_N = \mathcal{O}(N^{-\frac{1}{d}})$.*

Proof. Since X is a d-dimensional domain, there exists $c > 0$ such that $W_2(\mathrm{Leb}, \nu_N) \geq cN^{-\frac{1}{d}}$ for any measure ν_N supported at N points of $\mathbb{R}^d$. (Recall that, in this paper, Leb denotes the Lebesgue measure restricted to the set X, and normalized for unit mass.) The first point follows: for any measure μ_N supported at N points of $\mathbb{H}$

$$cN^{-\frac{1}{d}} \leq W_2(\mathrm{Leb}, \mathrm{e}_0 \#\mu_N) = W_2(\mathrm{e}_0 \#\mu, \mathrm{e}_0 \#\mu_N) \leq C_{\mathrm{e}} W_2(\mu, \mu_N) = C_{\mathrm{e}} h_N.$$

Second point: for each $x \in X$, let $\omega_x : t \mapsto s(t,x)$. Then $\Phi : (X, \mathrm{Leb}) \to (\Gamma, \mu) : x \mapsto \omega_x$ is measure preserving and Lipschitz, with regularity constant denoted C_Φ. Let ν_N be a discrete probability measure, with one Dirac mass of weight $1/N$ in each region of the partition $\mathcal{P}_N$. Since these regions have diameter $\leq C_{\mathcal{P}} N^{-\frac{1}{d}}$, we conclude that

$$h_N \leq W_2(\mu, \Phi\#\nu_N) = W_2(\Phi\#\,\mathrm{Leb}, \Phi\#\nu_N) \leq C_\Phi W_2(\mathrm{Leb}, \nu_N) \leq C_\Phi C_{\mathcal{P}} N^{-\frac{1}{d}}. \qquad \square$$

In the rest of this section, we fix the integer N and allow ourselves a slight abuse of notation: elements $\omega_j, P_j, \rho_j, \ldots$ indexed by $1 \leq j \leq N$ do implicitly depend on N, although that second index $\omega_j^N, P_j^N, \rho_j^N, \ldots$ is omitted for readability.

Lemma 3.6. *The infimum defining h_N is attained, see Definition 3.1. As a result there exists $(\omega_j)_{j=1}^N \in \mathbb{H}^N$ and probability measures $(\rho_j)_{j=1}^N$ on Γ such that*

$$\mu = \frac{1}{N} \sum_{1 \leq j \leq N} \rho_j \qquad\qquad h_N^2 = \frac{1}{N} \sum_{1 \leq j \leq N} \int_\Gamma \|\omega - \omega_j\|_{\mathbb{H}}^2 \, d\rho_j(\omega) \tag{17}$$

Furthermore, ω_j is the barycenter of ρ_j for each $1 \leq j \leq N$.

Proof. Let $(\omega_j)_{j=1}^N$ be a candidate quantization, and let π be the transport plan associated to $W_2^2(\frac{1}{N}\sum_{j=1}^N \delta_{\omega_j}, \mu)$. Then the measures $\rho_j : A \mapsto N\,\pi(\{x_j\} \times A)$, $1 \leq j \leq N$, are probabilities which average to μ, and the transport cost is the RHS of (17). The quantization energy, i.e. the squared Wasserstein distance, is decreased by replacing ω_j with the barycenter b_j of ρ_j, $1 \leq j \leq N$, by the amount $\frac{1}{N}\sum_{j=1}^N |\omega_j - b_i|^2$. Hence $\omega_j = b_j$ for all $1 \leq j \leq N$ if the quantization is optimal. Note also that the barycenter of ρ_j belongs to $G := \overline{\mathrm{Hull}(\Gamma)}$ by construction.

Since Γ is a compact subset of a Hilbert space, the convex hull closure G is also compact, for the strong topology induced by $\|\cdot\|_{\mathbb{H}}$. The quantization energy $(\omega_j)_{j=1}^N \mapsto W_2^2(\frac{1}{N}\sum_{j=1}^N \delta_{\omega_j}, \mu)$ attains its minimum on G^N by compactness, and by the previous argument it is the global minimum on $\mathbb{H}^N$. □

Let μ_N denote the equidistributed probability on the set $\{\omega_j;\ 1 \le j \le N\}$ of Lemma 3.6.

Lemma 3.7. *The regions of the partition $\mathcal{P}_N$ of Ω can be indexed as $(P_j)_{j=1}^N$ in such way that*

$$Ch_N^2 \ge \sum_{1\le j\le N} \int_{P_j} |\omega_j(0) - x|^2 dx. \tag{18}$$

Proof. Let $B_N \subseteq \Omega$ collect the barycenters of the partition $\mathcal{P}_N$, and let ν_N denote the equidistributed probability on B_N. One has

$$W_2(\nu_N, \mathrm{Leb}) \le C_{\mathcal{P}} N^{-\frac{1}{d}}, \qquad W_2(\mathrm{Leb}, \mathrm{e}_0 \#\mu_N) \le C_{\mathrm{e}} W_2(\mu, \mu_N) = C_{\mathrm{e}} h_N.$$

Thus $W_2(\nu_N, \mathrm{e}_0 \#\mu_N) \le C_1 h_N$ by Lemma 3.5. This optimal transport problem between the discrete measures ν_N and $\mathrm{e}_0 \#\mu_N$ determines an optimal assignment $\Gamma_N \to B_N$, represented by the indexation $(b_j)_{j=1}^N$ of Γ_N and B_N. Denoting by $P_j \in \mathcal{P}_N$ the region of which b_j is the barycenter we conclude that

$$\sum_{1\le j\le N} \int_{P_j} |\omega_j(0) - x|^2 dx = \sum_{1\le j\le N} \int_{P_j} |b_j - x|^2 dx + W_2^2(\nu_N, \mathrm{e}_0 \#\mu_N) \le Ch_N^2. \qquad \square$$

For each $0 \le i \le T$, let $m_i \in \mathbb{N}$ be the piecewise constant map on the partition $\mathcal{P}_N$ defined by

$$\forall 1 \le j \le N,\ \forall x \in P_j,\ m_i(x) := \omega_j(i/T).$$

Bound on the energy terms $\|m_{i+1} - m_i\|$. Using Cauchy-Schwartz's inequality we obtain

$$T \sum_{0\le i<T} \|m_{i+1} - m_i\|^2 = \frac{1}{N} \sum_{1\le j\le N} T \sum_{0\le i<T} \left|\omega_j\left(\frac{i+1}{T}\right) - \omega_j\left(\frac{i}{T}\right)\right|^2 \le \frac{1}{N} \sum_{1\le j\le N} \int_0^1 |\dot\omega_j(t)|^2 dt$$
$$= \frac{1}{N} \sum_{1\le j\le N} \int_0^1 \left|\int_\Gamma \dot\omega \, d\rho_j(\omega)\right|^2 \le \frac{1}{N} \sum_{1\le j\le N} \int_0^1 \int_\Gamma |\dot\omega|^2 \, d\rho_j(\omega)\, dt = d^2(s_*, s^*).$$

Distance to incompressible maps. For any $1 \le i \le T$, with $t := i/T$, one has

$$\inf_{s\in\mathbb{S}} \|m_i - s\| = W_2(\mathrm{Leb}, \mathrm{e}_t \#\mu_N) = W_2(\mathrm{e}_t \#\mu, \mathrm{e}_t \#\mu_N) \le C_{\mathrm{e}} W_2(\mu, \mu_N) = C_{\mathrm{e}} h_N.$$

Boundary conditions. We make the assumption that $s_* = \mathrm{Id}$, up to a minor modification of Lemma 3.7 (replace x with $s_*(x)$ in (18)). Lemma 3.7 then precisely states that $\|m_0 - s_*\|^2 \le Ch_N^2$, and the generalized boundary condition of (3) states that $\omega(1) = s^*(\omega(0))$ for μ-almost every $\omega \in \Gamma$. Denoting by C_0 the Lipschitz regularity constant of s^* we obtain for any $1 \le j \le N$ and $x \in X$

$$|\omega_j(1) - s^*(x)|^2 = \left|\int_\Gamma s^*(\omega(0)) - s^*(x)\, d\rho_j(\omega)\right|^2 \le \int_\Gamma |s^*(\omega(0)) - s^*(x)|^2 \, d\rho_j(\omega)$$
$$\le C_0^2 \int_\Gamma |\omega(0) - x|^2 \, d\rho_j(\omega) \le 2C_0^2 \left(\int_\Gamma |\omega_j(0) - \omega(0)|^2 \, d\rho_j(\omega) + |\omega_j(0) - x|^2\right).$$

Therefore

$$\begin{aligned}\|m_T - s^*\|^2 &= \sum_{1\le j\le N}\int_{P_j} |\omega_j(1) - s^*(x)|^2\,dx \\ &\le 2C_0^2 \sum_{1\le j\le N}\left(\frac{1}{N}\int_\Gamma |\omega_j(0)-\omega(0)|^2\,d\rho_j(\omega) + \int_{P_j}|\omega_j(0)-x|^2\,dx\right)\\ &\le 2C_0^2(C_{\mathrm{e}}^2 W_2^2(\mu_N,\mu) + \|m_0 - s_*\|^2) \le Ch_N^2.\end{aligned}$$

Summation and final estimate. The value $\mathcal{E}(T,N,\lambda)$ of the minimum (6) is

$$T\sum_{0\le i<T}\|m_{i+1}-m_i\|^2 + \lambda\left(\|m_0-s_*\|^2 + \|m_T - s^*\|^2 + \sum_{1\le i<T}\inf_{s\in\mathbb{S}}\|m_i - s\|^2\right) \le d^2(s_*,s^*) + \mathcal{O}(Th_N^2\lambda).$$

4 Numerical experiments

4.1 Minimization algorithm and choice of penalization

We rely on a quasi-Newton method to compute a (local) minimum of the discretized problem (6). This means that we need to compute the value of the functional

$$m\in\mathbb{M}_N^{T+1} \mapsto T\sum_{0\le i<T}\|m_{i+1}-m_i\|^2 + \lambda\Big(\|m_0-s_*\|^2 + \|m_T-s^*\|^2 + \sum_{1\le i<T} d_{\mathbb{S}}^2(m_i)\Big). \tag{19}$$

and its gradient, where $d_{\mathbb{S}}^2(m) = \inf_{s\in\mathbb{S}}\|m-s\|^2$. The only difficulty is to evaluate the squared distance $d_{\mathbb{S}}^2$ to the set of measure-preserving vector fields and its gradient. As explained in the introduction, Brenier's Polar Factorization Theorem implies that for any vector valued function $m\in\mathbb{M}$,

$$d_{\mathbb{S}}^2(m) = W_2^2(m\#\,\mathrm{Leb},\mathrm{Leb}).$$

When m belongs to $\mathbb{M}_N$, the measure $m\#\,\mathrm{Leb}$ is finitely supported, and the computation of the Wasserstein distance can be performed using a semi-discrete optimal transport solver [AHA98, Mer11, Lév14]. The next proposition gives an explicit formulation for the gradient in term of the optimal transport plan. Recall that $\mathbb{M}_N$ is the set of piecewise constant functions on the tessellation $\mathcal{P}_N := (P_j)_{1\le j\le N}$ of X. The diagonal $\mathbb{D}_N$ in $\mathbb{M}_N$ is the set of functions m in $\mathbb{M}_N$ such that $m(P_j) = m(P_k)$ for some $j\neq k$. The set $\mathbb{M}_N\setminus\mathbb{D}_N$ is a dense open set in $\mathbb{M}_N$.

Proposition 4.1. *The functional $d_{\mathbb{S}}^2$ is differentiable almost everywhere on $\mathbb{M}_N$ and continuously differentiable on $\mathbb{M}_N\setminus\mathbb{D}_N$. The gradient of $d_{\mathbb{S}}^2$ at $m\in\mathbb{M}_N\setminus\mathbb{D}_N$ is explicit: with $x_j = m(P_j)$,*

$$\nabla d_{\mathbb{S}}^2(m)\big|_{P_j} = 2(x_j - \mathrm{bary}(T^{-1}(x_j))) \tag{20}$$

where $T: X\to m(X)$ is the piecewise constant optimal transport map between Leb *and the finitely supported measure $m\#\,\mathrm{Leb}$ and* $\mathrm{bary}(S) = \int_S x dx/\,\mathrm{Leb}(S)$ *is the isobarycenter of S*

Proof. The functional $\mathcal{F} := d_{\mathbb{S}}^2 - \|\cdot\|^2$ is concave as an infimum of linear functions:

$$\mathcal{F}(m) = d_{\mathbb{S}}^2(m) - \|m\|^2 = \inf_{s\in\mathbb{S}}\|m-s\|^2 - \|m\|^2 = \inf_{s\in\mathbb{S}}\left[-2\langle m|s\rangle + \|s\|^2\right],$$

where $\langle \cdot, \cdot \rangle$ denotes the $L^2(X)$ scalar product. This implies in particular that $\mathcal{F}$ and therefore $d_{\mathbb{S}}^2$ is differentiable almost everywhere on $\mathbb{M}_N$. Given m in $\mathbb{M}_N \setminus \mathbb{D}_N$, define $x_j = m(P_j)$ and let $T : X \to \mathbb{R}^d$ be the optimal transport plan from Leb to $m\#\operatorname{Leb} = \frac{1}{N}\sum_{j=1}^N \delta_{x_j}$. The transport plan is indeed always representable by a function when the source measure is absolutely continuous with respect to the Lebesgue measure. Let $V_j = T^{-1}(x_j)$ be the partition of X induced by this transport plan. Then

$$\begin{aligned}\mathcal{F}(m) = W_2^2(m\#\operatorname{Leb}, \operatorname{Leb}) - \|m\|^2 &= \sum_{j=1}^N \int_{V_j} \|x_j - x\|^2 - \|x_j\|^2 dx \\ &= \langle m | G(m) \rangle + \sum_{j=1}^N \int_{V_j} \|x\|^2 dx\end{aligned}$$

where $G(m) \in \mathbb{M}_N$ is the piecewise constant function on X given by $G(m)|_{P_j} = -2\operatorname{bary}(V_j)$. For any m' in $\mathbb{M}_N$ and $x'_j = m'(V_j)$, one has

$$\begin{aligned}\mathcal{F}(m') = W_2^2(m'\#\operatorname{Leb}, \operatorname{Leb}) - \|m'\|^2 &\leq \sum_{j=1}^N \int_{V_j} \|x'_j - x\|^2 - \|x'_j\|^2 dx \\ &= \mathcal{F}(m) + \langle m' - m | G(m) \rangle\end{aligned}$$

This shows that $G(m)$ belongs to the superdifferential to $\mathcal{F}$ at m. In addition, by the continuity of optimal transport plans, the map $m \in \mathbb{M}_N \setminus \mathbb{D}_N \mapsto G(m)$ is continuous. To summarize, on the open domain $\mathbb{M}_N \setminus \mathbb{D}_N$ the concave function $\mathcal{F}$ possesses a continuous selection of supergradient. This implies that $\mathcal{F}$ is of class $\mathcal{C}^1$ on this domain, with $\nabla F(m) = G$, and the result follows. $\square$

Construction of the initial solution Since the discrete energy (19) is non-convex, the construction of the inital guess is important. We follow a time-refinement strategy already used by Brenier [Bre08] to construct a good initial guess. Assuming that we have already a local minimizer for $T_k = 2^k + 1$, we use linear interpolation to construct an initial guess for $T_{k+1} = 2^{k+1} + 1$. The optimization is then performed from this inital guess, using a quasi-Newton algorithm for the energy (19).

Choice of the penalization parameter The optimal choice of λ in (19) depends on the quantization dimension $D = D_{\text{quant}}(\mu)$ of the generalized solution $\mu \in \operatorname{Prob}(\Omega)$ that one expects to recover: namely $\lambda_N = N^{-\frac{1}{D}}$, see the remark after (11). We call D the flow dimension, and regard it as as the intrinsic dimensionality of the problem which determines its computational difficulty. For a classical solution, this dimension agrees with the ambient dimension i.e. $D = d$, while for a non-deterministic solution the quantization dimension can be up to $2d$. Intermediate dimensions $d < D < 2d$ are also common [Bre89]. In our numerical experiments we set $\lambda_N = N^{\frac{1}{3}}$, a decision justified a-posteriori by the numerical estimation of the quantization dimension of the computed solution, see Figure 9.

Note that the numerical error in (11) is governed (for a fixed number T of time steps) by the quantity $\lambda^{-1} + h_N^2 \lambda$, and that $h_N = \mathcal{O}(N^{-\frac{1}{2d}})$ under the assumptions of Theorem 1.1. The choice $\lambda_N = N^{\frac{1}{\alpha}}$ thus yields a convergent scheme whenever $\alpha > d$, although convergence rates are improved if α is close to the flow dimension D, so that $\lambda_N \approx N^{\frac{1}{D}} \approx h_N^{-1}$.

4.2 Visualization of generalized solution

The main interest of numerical experimentation is to visualize generalized solutions to Euler's equation, or equivalently generalized geodesics between two measure-preserving diffeomorphisms s_*, s^* in $\mathbb{S}$.

4.2.1 Gradient of the pressure

Consider a minimizer of the discretized energy (19). Given $i \in \{1, \dots, T-1\}$, m_i minimizes over $\mathbb{M}_N$ the functional $m \mapsto T(\|m - m_{i-1}\|^2 + \|m_{i+1} - m\|^2) + \lambda d^2_{\mathcal{S}}(m)$. This gives

$$T^2(m_{i-1} - 2m_i + m_{i+1}) = T\lambda \nabla d^2_{\mathcal{S}}(m_i). \tag{21}$$

This equation is a discretized counterpart of the rule that the acceleration of a geodesic on an embedded manifold, is normal to that manifold (here $\mathbb{S}$ plays the role of the manifold, embedded in $\mathbb{M}$, which is internally approximated by the linear space $\mathbb{M}_N$). The second order difference $T^2(m_{i-1} - 2m_i + m_{i+1})$ approximates a second derivative in time. Comparing (21) to (4), we see that the right hand-side of (21) can be used as an estimation of (minus) the pressure of the gradient.

4.2.2 Geometric data analysis

As in the proof of Theorem 1.1, the discrete minimizer of (19) can converted to a collection of N piecewise-linear curves $\{\omega_1, \dots, \omega_N\} = \Gamma_N$. We recall that the domain X is partitioned into N subdomains $(P_j)_{1 \leq j \leq N}$ with equal area and we let $\omega_j(i/T) \in \mathbb{R}^d$ be the point corresponding to the restriction of m_i to the subdomain P_j, for each $0 \leq i \leq T$. Figure 3 illustrates this construction. We regard Γ_N as embedded in the Hilbert space $\mathbb{H} := H^1([0,1], \mathbb{R}^2)$ which plays a natural role in the problem of interest, as in §3, and apply techniques from the field of geometric data analysis.

Clustering In order to better visualize the solution, we use the k-means algorithm to divide the set Γ_N into k. A distinct particle color is attached to each cluster, see for instance Figure 6. The k-means algorithm consists in finding a local minimizer of the optimal quantization problem

$$\min_{\ell_1, \dots \ell_k \in \mathbb{H}} \frac{1}{N} \sum_{\omega \in \Gamma_N} \min_{1 \leq i \leq k} \|\omega - \ell_i\|^2_{\mathbb{H}} \tag{22}$$

using a simple fixed point algorithm, and to divide Γ_N into clusters $(C_i)_{1 \leq i \leq k}$ with

$$C_i = \left\{ \omega \in \Gamma_N ; \|\omega - \ell_i\|_{\mathbb{H}} = \arg\min_{1 \leq j \leq k} \|\omega - \ell_i\|_{\mathbb{H}} \right\}.$$

Note that $l_1, \cdots, l_k$ automatically belong to $\mathrm{Span}(\Gamma_N)$, hence to the $d(T+1)$-dimensional linear subspace of $\mathbb{H}$ consisting of piecewise linear paths with nodes $\omega(t) \in \mathbb{R}^d$ at times $t = i/T$, $0 \leq i \leq T$. This makes (22) tractable.

Box dimension A natural objective is to estimate the quantization dimension $D_{\mathrm{quant}}(\mu)$ of the generalized flow $\mu \in \mathrm{Prob}(\Omega)$ minimizing the relaxed problem (3). The probability measure μ_N equidistributed on the set Γ_N approximates μ, see Proposition 1.2, hence we can expect the set Γ_N to also approximate $\mathrm{supp}(\mu)$. The quantization dimension $D_{\mathrm{quant}}(\mu)$ is difficult to

estimate, but by Proposition 3.2 it admits the simpler upper bound $D_{\text{box}}(\text{supp}(\mu))$. We estimate the latter by applying the furthest point sampling algorithm to the finite metric space Γ_N, which defines an ordering on the elements of Γ_N as follows: let γ_1 be an arbitrary point of Γ_N and define by induction

$$\gamma_{i+1} := \arg\max_{\gamma\in\Gamma_N} d(\gamma, \{\gamma_1, \dots, \gamma_i\}) \tag{23}$$

As in Definition 3.1, denote by $r_i = r_i(\Gamma_N)$ is the smallest $r \geq 0$ such that Γ_N can be covered by i balls of radius r. For $1 \ll i \ll N$, the ratio $\log(i)/\log(1/r_i(\Gamma_N))$ is expected to approximate $\log(i)/\log(1/r_i(\text{supp}(\mu)))$ and thus the desired $D_{\text{box}}(\text{supp}\,\mu)$.

Lemma 4.2. *Let $\varepsilon_i := \max_{\gamma\in\Gamma} d(\gamma, \{\gamma_1, \dots, \gamma_i\})$, where γ_i is defined as in (23). Then,*

$$\left(1 - \frac{\log(2)}{\log(1/\varepsilon_i)}\right) \frac{\log(i)}{\log(1/\varepsilon_i)} \leq \frac{\log(i)}{\log(1/r_i)} \leq \frac{\log(i)}{\log(1/\varepsilon_i)}$$

Proof. By construction, $r_i \leq \varepsilon_i$. Moreover, the balls centered at the points $\gamma_1, \dots, \gamma_i$ and with radius $\varepsilon_i/2$ are disjoint, so that $r_i \geq \varepsilon_i/2$. □

4.3 Test cases and numerical results

Our two testcases are constructed from two stationary solutions to Euler's equation in 2D. Let $s : \mathbb{R}_+ \to \mathbb{S}$ be a classical solution to Euler equation in Lagrangian coordinates (4), starting from the identity map. We solve the discretized version (6) of the minimization problem (2)-(3), with $s_* = s(0) = \text{Id}$ and $s^* := s(t_{\max})$, where $t_{\max} > 0$. For small values of $t_{\max}$ the solution to this boundary problem is simply the original classical flow s, but for larger values a completely different generalized flow is obtained. In this case the geodesic s in the space of the measure preserving diffeomorphisms is no longer the unique shortest path between its boundary values s_* and s^*. The first classical behavior is guaranteed if the pressure hessian satisfies

$$\nabla^2 p \prec (\pi/t_{\max})^2 \,\text{Id} \tag{24}$$

uniformly on $[0, t_{\max}] \times X$, see (5) and [Bre89]. In all the numerical experiments, the number of points is set to $N = 10\,000$ and the number of timesteps is $T = 2^4 + 1 = 17$.

4.3.1 Rotation of the disk

On the unit disk $D = \{(x_1, x_2) \in \mathbb{R}^2;\, x_1^2 + x_2^2 \leq 1\}$, the simplest stationary solution to Euler's equation (1) is given by a time-independent pressure field and speed:

$$p(x_1, x_2) = \frac{1}{2}(x_1^2 + x_2^2), \qquad\qquad v(x_1, x_2) = (-x_2, x_1).$$

The corresponding Lagrangian flow $s(t)$ is simply the rotation of angle t. The largest eigenvalue of $\nabla^2 p$ is 1 at every point in D. Hence by (24) the flow of rotations is the unique minimizer to both the variational formulation (2) and its relaxation (3) with boundary values $s_* = s(0) = \text{Id}$ and $s^* = s(t_{\max})$, when $t_{\max} < \pi$. Uniqueness is lost at the critical time $t_{\max} = \pi$ which corresponds to a rotation of angle π, so that the final diffeomorphism becomes $s_* = s(\pi) = -\,\text{Id}$. In this situation, the minimization problem (2) has two classical solutions, namely the clockwise and counterclockwise rotations. The relaxation (3) has uncountably many generalized solutions such as, by linearity, superpositions of these two rotations.

Another explicit example of generalized solution was discovered by Brenier [Bre89]: given a point $x \in D$ and a speed v, denote by $\omega_{x,v}$ the curve $\omega_{x,v}(t) = x\cos(t) + v\sin(t)$, $t \in [0, 1]$. Then,

Brenier's solution is obtained as the pushforward by the map $(x, v) \mapsto \omega_{x,v} \in \Omega$ of the measure on $D \times \mathbb{R}^2$ defined by

$$\mu(dx, dv) = \frac{1}{\pi}\mathcal{H}^2(dx) \otimes \frac{1}{2\pi\sqrt{1-|x|^2}}\, \mathcal{H}^1\big|_{\{|v|=\sqrt{1-|x|^2}\}}(dv),$$

where $\mathcal{H}^k$ denotes the k-dimensional Hausdorff measure. In particular, the quantization dimension of the solution is $3 = 2 + 1$. We refer to [BFS09] for more examples of optimal flows, and construct four dimensional one. Let μ_r be defined by combining (i) a classical rotation on the annulus $D \setminus D(r)$, with $D(r) = \{x \in \mathbb{R}^2;\, |x| \leq r\}$ and (ii) Brenier's solution rescaled by a factor r on the disc $D(r)$. Then μ_r is an optimal generalized flow of quantization dimension 3, whereas the averaged flow $\int_0^1 \mu_r dr$ is also optimal by linearity, and has quantization dimension 4.

Numerical results The numerical solutions computed by our algorithm for the critical time $t_{\max} = \pi$ are highly non-deterministic. To see this, we select a small neighborhood around several points in the unit disk D and look at the trajectories emanating from this small neighborhood. As shown in Figure 8, we can see that the trajectories emanating from each neighborhood fill up the disk. In addition, each indivual trajectory looks like an ellipse. Second, we estimate the box dimension of the support of the numerical solution (as explained in §4.2). The estimated dimension is slightly above 3.

4.3.2 Beltrami flow on the square

On the unit square $S = [-1/2, 1/2]^2$, we consider the Beltrami flow constructed from the time-independent pressure and speed:

$$\begin{aligned} p(x_1, x_2) &= \frac{1}{2}(\sin(\pi x_1)^2 + \sin(\pi x_2)^2) \\ v(x_1, x_2) &= (-\cos(\pi x_1)\sin(\pi x_2), \sin(\pi x_1)\cos(\pi x_2)) \end{aligned}$$

The maximum eigenvalue of $\nabla^2 p$ is π^2, and [Bre89] implies that the associated flow is minimizing between $s_* = s(0) = \mathrm{Id}$ and $s^* = s(t_{\max})$ for $t_{\max} \leq 1$. Because of the lack of symmetry, generalized solutions constructed from this flow are less understood than in the disk case.

Numerical results Our numerical results suggest the following observations. First, as shown in Figure 5, the computed solutions with boundary values $s_* = \mathrm{Id}$ and $s^* = s(t_{\max})$ approximate the classical flow if $t_{\max} < 1$, and are non-deterministic generalized flows if $t_{\max} \geq 1$. This suggests the sharpness of the bound given by [Bre89]. Interestingly, even for $t > 1$, the numerical solutions seem to remain deterministic in a neighborhood of the boundary of the cube. This can be seen more clearly in Figure 6, where the particles have been divided into clusters using the k-means algorithm (see §4.2.2).

The pressure gradient is estimated as in §4.2.1 and is displayed in Figure 7. These pictures seem to indicate a loss of regularity of the pressure near the initial and final times. This corroborates the result of [AF07] according to which the pressure belongs to $L^2_{\mathrm{loc}}(\,]0, T[,\, \mathrm{BV}(X))$.

Figure 8 suggests that the even for $t_{\max} = 1.5$, the reconstructed solution for the Beltrami flow are more deterministic than the solution to the disk inversion. We estimate the box dimension of the support of the solution using the method explained in §4.2.2. The result are displayed in Figure 9. The estimated dimension is $D = 2$ for the deterministic solution ($t_{\max} = 0.9$) but it increases as the maximum time (and therefore the amount of non-determinism) increases.

Finally, we note that the estimated dimensions for $t_{\max} \in \{1.1, 1.3, 1.5\}$ seem to be strictly between 2 and 3, suggesting a fractal structure for the support of the solution. This would need to be confirmed by a mathematical study.

Software. The software developed for generating the results presented in this article is publicly available at `https://github.com/mrgt/EulerSemidiscrete`

Acknowledgement The authors thank Y. Brenier for constructive discussions and introducing them to the topic of Euler equations of inviscid incompressible fluids.

References

[AF07] Luigi Ambrosio and Alessio Figalli. On the regularity of the pressure field of Brenier's weak solutions to incompressible Euler equations. *Calculus of Variations and Partial Differential Equations*, 2007.

[AHA98] F Aurenhammer, F Hoffmann, and B Aronov. Minkowski-Type Theorems and Least-Squares Clustering. *Algorithmica*, 1998.

[Arn66] Vladimir Arnold. Sur la géométrie différentielle des groupes de Lie de dimension infinie et ses applications à l'hydrodynamique des fluides parfaits. *Annales de l'institut Fourier*, 1966.

[BCMO14] Jean-David Benamou, Guillaume Carlier, Q Merigot, and Edouard Oudet. Discretization of functionals involving the Monge-Ampère operator. *arXiv.org*, 2014.

[BFS09] Marc Bernot, Alessio Figalli, and Filippo Santambrogio. Generalized solutions for the Euler equations in one and two dimensions. *Journal de Mathématiques Pures et Appliquées*, 2009.

[Bre89] Yann Brenier. The least action principle and the related concept of generalized flows for incompressible perfect fluids. *Journal of the American Mathematical Society*, 1989.

[Bre91] Yann Brenier. Polar factorization and monotone rearrangement of vector-valued functions. *Communications on Pure and Applied Mathematics*, 1991.

[Bre93] Y Brenier. The dual least action principle for an ideal, incompressible fluid. *Archive for rational mechanics and analysis*, 1993.

[Bre08] Yann Brenier. Generalized solutions and hydrostatic approximation of the Euler equations. *Physica D. Nonlinear Phenomena*, 2008.

[Bre11] Yann Brenier. A modified least action principle allowing mass concentrations for the early universe reconstruction problem. *Confluentes Mathematici*, 2011.

[cga] CGAL, Computational Geometry Algorithms Library. http://www.cgal.org.

[Eul65] Leonhard Euler. *Opera Omnia*. 1765.

[FD12] Alessio Figalli and S Daneri. Variational models for the incompressible Euler equations. *HCDTE Lecture Notes, Part II*, 2012.

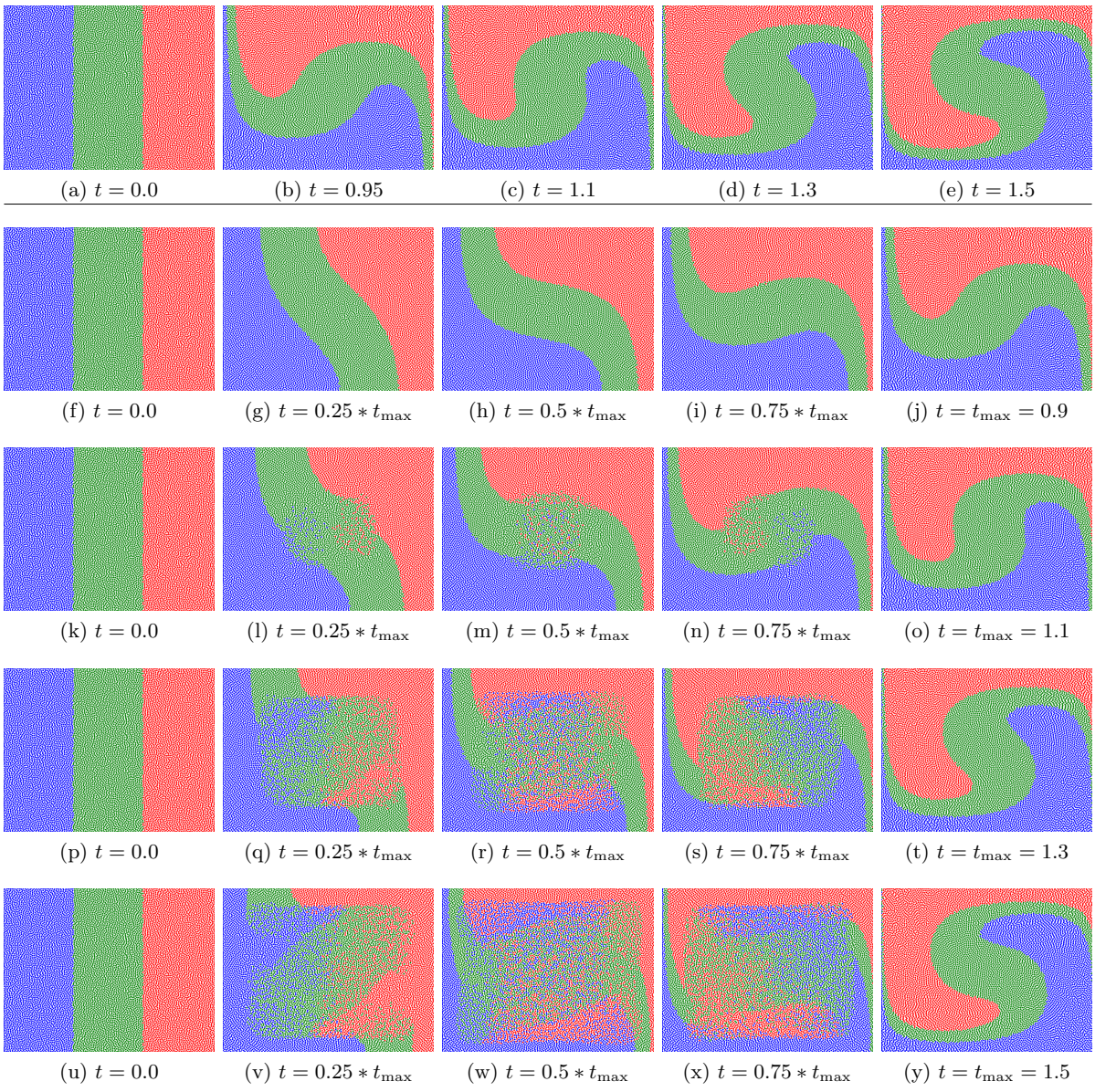

(a) $t = 0.0$ (b) $t = 0.95$ (c) $t = 1.1$ (d) $t = 1.3$ (e) $t = 1.5$

(f) $t = 0.0$ (g) $t = 0.25 * t_{\max}$ (h) $t = 0.5 * t_{\max}$ (i) $t = 0.75 * t_{\max}$ (j) $t = t_{\max} = 0.9$

(k) $t = 0.0$ (l) $t = 0.25 * t_{\max}$ (m) $t = 0.5 * t_{\max}$ (n) $t = 0.75 * t_{\max}$ (o) $t = t_{\max} = 1.1$

(p) $t = 0.0$ (q) $t = 0.25 * t_{\max}$ (r) $t = 0.5 * t_{\max}$ (s) $t = 0.75 * t_{\max}$ (t) $t = t_{\max} = 1.3$

(u) $t = 0.0$ (v) $t = 0.25 * t_{\max}$ (w) $t = 0.5 * t_{\max}$ (x) $t = 0.75 * t_{\max}$ (y) $t = t_{\max} = 1.5$

Figure 5: *(First row)* Beltrami flow in the unit square at various timesteps, a classical solution to Euler's equation. The color of the particles depend on their initial position. *(Second to fifth row)* Generalized fluid flows that are reconstructed by our algorithm, using boundary conditions displayed in the first and last column. When $t_{\max} < 1$ we recover the classical flow, while for $t_{\max} \geq 1$ the solution is not classical any more and includes some mixing.

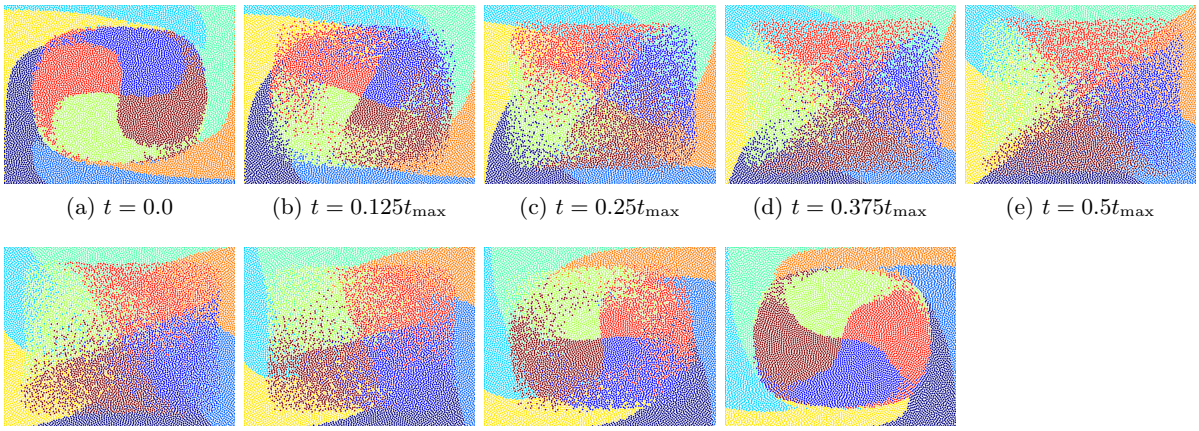

(a) $t = 0.0$ (b) $t = 0.125t_{\max}$ (c) $t = 0.25t_{\max}$ (d) $t = 0.375t_{\max}$ (e) $t = 0.5t_{\max}$

(f) $t = 0.625t_{\max}$ (g) $t = 0.75t_{\max}$ (h) $t = 0.875t_{\max}$ (i) $t = t_{\max} = 1.5$

Figure 6: Using the k-means cluster algorithm, we cluster the reconstructed trajectories for the Beltrami flow in the square with $t_{\max} = 1.5$ into 10 groups. This suggests that close to the boundary of the square the movement of particle is clockwise and deterministic while in the interior the movement is highly non-deterministic and counter-clockwise.

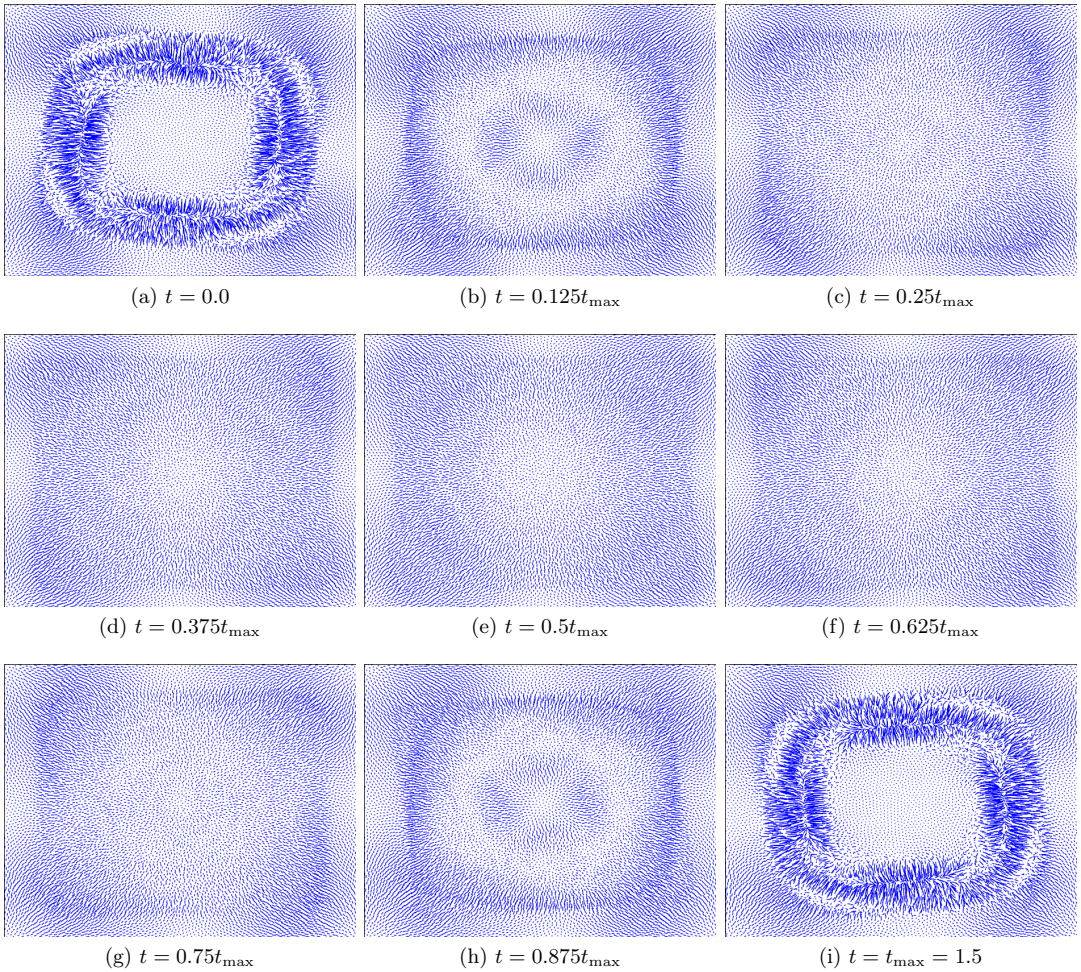

(a) $t = 0.0$ (b) $t = 0.125t_{\max}$ (c) $t = 0.25t_{\max}$

(d) $t = 0.375t_{\max}$ (e) $t = 0.5t_{\max}$ (f) $t = 0.625t_{\max}$

(g) $t = 0.75t_{\max}$ (h) $t = 0.875t_{\max}$ (i) $t = t_{\max} = 1.5$

Figure 7: Estimated pressure gradient for the Beltrami flow on the square with $t_{\max} = 1.5$.

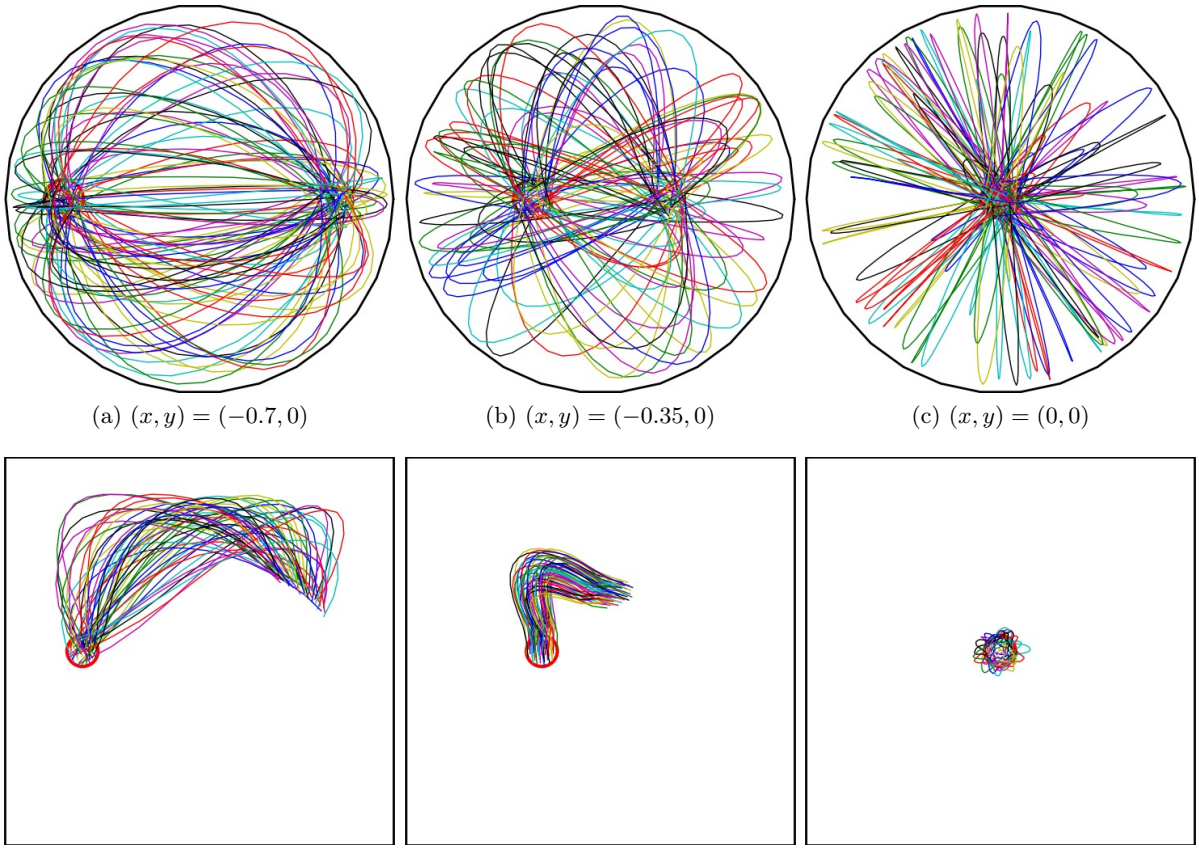

(a) $(x, y) = (-0.7, 0)$ (b) $(x, y) = (-0.35, 0)$ (c) $(x, y) = (0, 0)$

(d) $(x, y) = (0.2, 0)$ (e) $(x, y) = (0.35, 0)$ (f) $(x, y) = (0.5, 0)$

Figure 8: We select particles whose initial position lie in a small disk, and display their trajectories according to the computed solution to (19). (Top) For the inversion of the unit disk (Bottom) For the Beltrami flow on the square, with $t_{\max} = 1.5$.

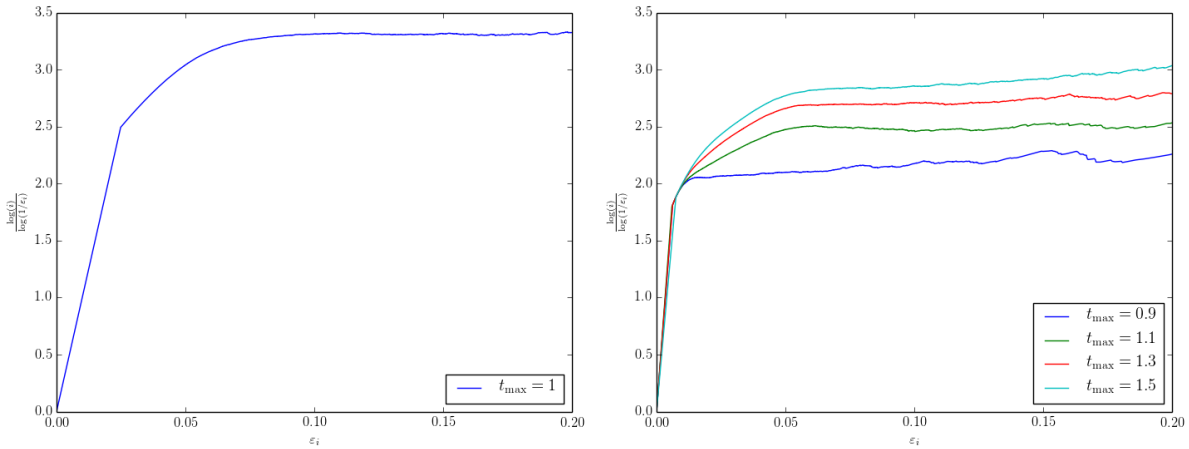

Figure 9: Estimation of the box counting dimension of the support of the computed solution, see §4.2.2. *(Left)* for the inversion of the unit disk *(Right)* Comparison between the estimated box counting dimensions of the solutions to the Beltrami flow on the square, depending on the maximum time.

[GG92] Allen Gersho and Robert M Gray. *Vector Quantization and Signal Compression.* Springer Science & Business Media, 1992.

[Lév14] Bruno Lévy. A numerical algorithm for L_2 semi-discrete optimal transport in 3D. *arXiv.org*, 2014.

[Mer11] Q Merigot. A Multiscale Approach to Optimal Transport. *Computer Graphics Forum*, 2011.

[Shn94] A I Shnirelman. Generalized fluid flows, their approximation and applications. *Geometric and Functional Analysis*, 1994.